

# Right Reward Right Time for Federated Learning

Thanh Linh Nguyen, Dinh Thai Hoang, Diep N. Nguyen, and Quoc-Viet Pham

**Abstract**—Critical learning periods (CLPs) in federated learning (FL) refer to early stages during which low-quality contributions (e.g., sparse training data availability, strategic non-participation) can permanently impair the performance of the global model owned by the model owner (i.e., a cloud server). However, existing incentive mechanisms typically exhibit temporal homogeneity, treating all training rounds as equally important, thereby failing to prioritize and attract high-quality contributions during CLPs. This inefficiency is compounded by information asymmetry due to privacy regulations, where the cloud lacks knowledge of client training capabilities, leading to adverse selection. Thus, in this article, we propose a time-aware contract-theoretic incentive framework, named Right Reward Right Time (R3T), to encourage client involvement, especially during CLPs, to maximize the utility of the cloud server in FL. We formulate a cloud utility function that captures the trade-off between the achieved model performance and rewards allocated for clients’ contributions, explicitly accounting for client heterogeneity in time and system capabilities, effort, and joining time. Then, we devise a CLP-aware incentive mechanism deriving an optimal contract design that satisfies individual rationality, incentive compatibility, and budget feasibility constraints, motivating rational clients to participate early and contribute efforts. By providing the right reward at the right time, our approach can attract the highest-quality contributions during CLPs. Simulation and proof-of-concept studies show that R3T mitigates information asymmetry, increases cloud utility, and yields superior economic efficiency than conventional incentive mechanisms benchmarks. Our proof-of-concept results demonstrate up to a 47.6% reduction in the total number of clients and up to a 300% improvement in convergence time while achieving competitive test accuracy.

**Index Terms**—Critical learning periods, Federated learning, Incentive mechanism, Blockchain, Contract theory.

## I. INTRODUCTION

### A. Background and Motivations

Federated learning (FL) is a privacy-preserving distributed learning paradigm, where distributed clients (e.g., devices or organizations) collaboratively train a shared artificial intelligence model under the coordination of a central server without disclosing private data [2], [3]. In classical FL settings, the importance of all training rounds and the efforts of distributed clients across these rounds are weighted equally. However, this setting is questioned by a recent finding in FL known as critical learning periods (CLPs), which highlight the varying impacts of different training rounds and significantly affect FL learning and training efficiency [4], [5]. This finding was inspired by earlier research on CLPs in species’ cognitive

Thanh Linh Nguyen and Quoc-Viet Pham are with the School of Computer Science and Statistics, Trinity College Dublin, The University of Dublin, Dublin 2, D02PN40, Ireland (e-mail: {tnguyen3, viet.pham}@tcd.ie).

Dinh Thai Hoang and Diep N. Nguyen are with the School of Electrical and Data Engineering, University of Technology Sydney, Sydney, NSW 2007, Australia (e-mail: {hoang.dinh, diep.nguyen}@uts.edu.au).

Part of this article was presented at the 2025 IEEE 101st Vehicular Technology Conference [1].

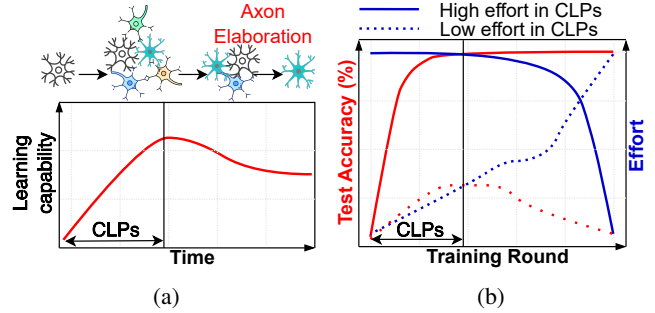


Fig. 1: Illustration of: a) CLPs in the biological field [13], and b) how early effort affects FL global model performance [4].

and learning functions (i.e., humans and animals) and deep learning networks within a centralized setting [6]–[9]. Particularly, CLPs are early learning phases (c.f., Fig. 1(a)) affecting long-term learning capabilities [10]. Empirical studies show that the absence of proper learning during these periods can lead to irreversible deficits. For instance, barn owls exposed to misaligned auditory and visual cues during their critical development periods fail to properly localize spatial locations in adulthood [11]. This phenomenon was also observed in deep neural networks, in which any deficits and low effort (e.g., sparse data availability, late client participation) during this initial learning stage can cause lasting impairment on model performance, regardless of subsequent efforts (c.f., Fig. 1(b)) [4], [12]. The reason for the phenomenon is still unclear, but possible explanations include the depth of the learning model, the structure of training data distribution, or defects in the implementation and training process [7]–[9].

Despite the promising merits of enhancing FL efficiency (e.g., accuracy and convergence rate), CLPs remain under-explored, including a lack of transparent, fair, and timely incentives for participation and contribution elicitation, and information asymmetry among clients and the global model owner (e.g., a cloud server<sup>1</sup>) during these periods. Existing CLP-considered works in FL, such as CLPs detection, client selection, or CLP-aware aggregation, are based on a common assumption of voluntary engagement of clients in the training process (e.g., [4], [5], [14], [15]). However, this is impractical because clients are *rational, strategic, benefit-driven*, and need sufficient rewards to compensate for their efforts (e.g., data, computation resources, and time costs). This leads to a lack of client motivation for contribution, resulting in the unsustainable development of FL systems. Although several works have been proposed to bring incentivization by considering effort-reward approaches to fairly compensate FL clients’ effort (e.g., [16]–[19]), they treat clients’ efforts and their impacts on the

<sup>1</sup>The cloud server and the cloud are used interchangeably.

global model performance on every training round equally and ignore the temporal factor, whereas efforts in CLPs have more weights and mainly contribute to the overall performance of the global model. By failing to prioritize CLP-driven incentive solutions, current methods inefficiently allocate cloud rewards (e.g., money), thereby reducing cloud utility—defined as the difference between gains from global model performance and compensation costs (which is defined later in Section II).

Furthermore, the design of efficient incentives is hindered by information asymmetry between the FL clients and the cloud server. Specifically, due to privacy restrictions, the cloud lacks prior knowledge of the clients' private training capabilities, including the data, communication, and computation resources, efforts (e.g., data quantity and distribution), or available joining time. Therefore, assumptions that the cloud server knows precise information [20]–[22], such as clients' computing resources or clients' data size, may not hold in practice. A compounded challenge overlooked by prior works is that existing contract-theoretic incentive approaches, while effective for handling information asymmetry in FL incentives (e.g., [23]), fail to incorporate the temporal heterogeneity of CLPs, where early deficits cause irreversible model impairments regardless of later efforts [4], [5]. This leads to suboptimal contract designs that treat all training rounds equally, inefficiently allocating incentives without prioritizing high-quality contributions<sup>2</sup> during CLPs, resulting in diluted contributions and permanent performance losses under asymmetry about clients' training capabilities.

There is also uncertainty regarding whether clients will exert the promised effort post-contract [24]. Even with contractually specified incentives, clients may engage in moral-hazard behaviors (e.g., low-effort training or strategic dropouts), and the cloud may be accused of delaying or renegeing on payments, which can lead to disputes. Addressing these issues requires costly monitoring and verification and remains error-prone, increasing the difficulty of sustaining FL and implementing fair incentive mechanisms [17]. In this article, we aim to address the following research question (RQ).

**RQ:** How can we design an incentive mechanism to attract rational clients with highest-quality contributions to improve FL learning and training efficiency, and mitigate information asymmetry between clients and the cloud, given the crucial role of CLPs in determining the final FL model performance?

To address the aforementioned challenges, we propose a *CLP-aware* incentive contract-theoretic framework, named **Right Reward Right Time** (R3T). Leveraging contract theory, R3T effectively mitigates the information asymmetry issues by designing a set of temporally integrated contract items for the cloud server [24]. The optimal contract design incentivizes clients to self-reveal their training capabilities, join early, and contribute efforts by optimally prioritizing and providing

<sup>2</sup>We refer to **high-quality contributions** to high training efforts, such as a huge amount of closer-distribution-to-the-learning-task data and large computation resources, and they are available in CLPs.

corresponding generous rewards in the early training phase under complete and incomplete information cases, while satisfying individual rationality, incentive compatibility, and budget feasibility constraints. By providing the right reward at the right time, R3T enables the highest-quality clients to join early and contribute efforts during CLPs. R3T also integrates with blockchain smart contracts to handle the issues of centralized incentive governance and disputes caused by relying on the cloud server [25]–[27].

### B. Related Work

In the following, we discuss related work concerning CLPs in artificial neural networks and incentive mechanisms.

*Critical learning periods in neural networks.* Achille et al. in [7] empirically investigated the correlation between critical periods in the memorization phase and the training outcome in deep neural networks. Their findings demonstrated that, analogous to animals, sensory deficits in CLPs cause lasting impairments to the information and connectivity of the network, as quantified by an approximation of the Fisher Information, and adversely affect learning outcomes regardless of subsequent additional training. Similarly, Kleinman et al. in [28] analytically found that the depth of the deep neural network model and data distribution structure are fundamental sources of CLPs in deep networks, not only being explained by ascribing to biological aging processes observed in animals. A similar pattern was found in the distributed training manner, where Yan et al. in [4], [14] showed that FL exhibits CLPs, which play a vital role in determining the final training performance, given the complexity of statistical and system heterogeneity. To further explain the phenomenon, metrics such as federated Fisher Information matrix and CLP-aware federated norm vector are proposed to trace and detect CLPs.

However, these CLP-aware FL studies assume voluntary participation and overlook costs and benefit-driven and strategic behavior, which do not reflect real-world conditions. Without proper CLP-target incentives, it may lead to the lack of high-quality contributions in CLPs that have been shown to be permanent and irrecoverable impairment on the global model performance, despite subsequent efforts.

*Incentive mechanisms.* By incorporating incentive mechanisms into FL systems, engagement and cooperation are promoted where clients are rational, resulting in enhanced efficiency [29]. Realizing the importance of incentive mechanisms, there are several efforts to develop game-theoretic incentive techniques in FL (e.g., [23], [30]–[35]). Authors in [30]–[32] designed leader-follower-based incentive mechanisms to encourage clients' contribution, where the cloud server sets the total reward or price per contribution unit, and then FL clients determine contribution strategies (e.g., data quantity or local performance) to maximize their utilities. However, the information asymmetry condition was not considered in these studies. To handle this issue, utilizing the self-revelation principle of contract theory [24], Sun et al. in [23] proposed an incentive mechanism using a single client's property (i.e., privacy leakage costs) to create different contract items under both complete and incomplete information cases

to compensate for client's privacy leakage while ensuring comparable learning model performance. Under the same information cases, Huang et al. in [34] proposed a data quality-based incentive mechanism, where the client's data size, data quality, and unit data computing cost are considered, to derive optimal contract items to optimize the cloud server's costs in the era of artificial intelligence-generated. Tang et al. in [35] proposed a non-cooperative game-based incentive mechanism to model the interactions between clients (i.e., organizations), deriving optimal processing capacity of each client, to address free-rider problems of public goods in FL under constraints of individual rationality and budget balance.

To provide further comprehensive incentive solutions by handling the transparency, centralization, and potential disputes among clients and the cloud server, blockchain is fused with FL systems to manage incentive calculation and distribution [32], [35]–[37]. For instance, Yuan et al. in [37] utilized Ethereum-based smart contracts to autonomously execute an incentive mechanism, that considers influences from competition and provides fair and non-repudiative compensation and incentive, to improve social welfare.

*Nevertheless, existing works on incentive mechanisms in FL to provide the right reward at the right time have not been explored yet. None of these works consider the existence of CLPs, which have been shown to play a vital role in determining final FL model performance, and these studies treat every training round as equally important. Besides, information asymmetries among clients and the cloud server, and their impacts on CLPs' advantages and the final model performance have not been analyzed yet.*

To the best of our knowledge, R3T is the first CLP-aware incentive mechanism, considering the joint importance of joining time and effort, to attract the highest-quality rational clients to participate in the FL model training in early stages and mitigate information asymmetry between clients and the cloud server. R3T provides a transparent and autonomous execution of reward calculation and distribution.

### C. Contributions

The main contributions of this paper are as follows:

- *Temporal-integrated contract-theoretic incentive framework:* We develop a *time-aware* contract-theoretic framework, named R3T, which is the first to explicitly integrate CLPs into FL incentive design. R3T characterizes cloud utility as a function of client time and system capability, effort, joining time, and reward decisions.
- *CLP-aware incentive mechanism design:* We develop a CLP-aware incentive mechanism that analytically derives an optimal contract to jointly optimize client participation strategies and cloud utility while adaptively attracting high-quality rational clients in the early training stages to enhance FL training and learning efficiency. The proposed incentive mechanism provides the right reward at the right time and handles issues of information asymmetries between clients and the cloud.
- *Performance evaluation:* We conduct simulations to verify the effectiveness of our R3T in information symmetry

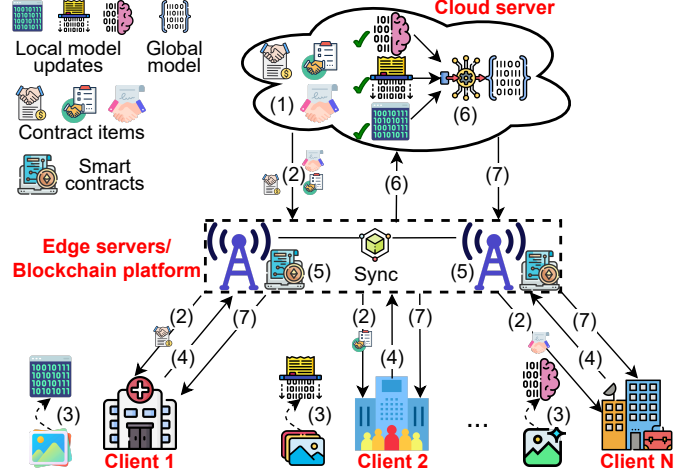


Fig. 2: R3T's one-round learning workflow: (1) prepare contracts, (2) sign contracts & download global model, (3) local training, (4) upload updates, (5) forward & validate updates, (6) receive & aggregate model updates, and (7) settlement.

and information asymmetry cases under individual rationality, incentive compatibility, and budget feasibility constraints. R3T demonstrates feasibility and superior efficiency compared with conventional incentive mechanism benchmarks, including linear pricing and conventional contract theory-based methods.

- *Proof of concept:* We implement a proof of concept of R3T and demonstrate the feasibility and efficiency of the proposed mechanism and system design. Significantly, we show that R3T can boost the convergence time by up to 300% while achieving competitive final FL model accuracies on standardized benchmark datasets, CIFAR-10 and Fashion-MNIST, compared with the state-of-the-art incentive mechanism benchmarks.

## II. SYSTEM MODEL

### A. System Overview

As depicted in Fig. 2, the R3T framework consists of three main components: edge servers forming a blockchain platform, clients, and a cloud server. We denote a set of edge servers as  $\mathcal{L}$ , where each edge server  $l \in \mathcal{L}$  connects with clients to exchange information.  $\mathcal{L}$  forms, maintains, and operates a blockchain platform to record and validate information such as client identification (ID), local model updates, global models, joining time, and effort levels. Also, R3T integrates a distributed file storage system such as InterPlanetary File System (IPFS), to achieve privacy preservation, high availability, scalability, and low latency for data storage and retrieval [38]. The set of clients is denoted as  $\mathcal{N} = \{1, \dots, n, \dots, N\}$ , where  $N$  represents the number of clients. Clients join and contribute their time, computing, and data resources to jointly train the global model published by the cloud server, in exchange for benefits such as monetary rewards. In each training round, a subset of clients  $\mathcal{S}_n \subseteq \mathcal{N}$  participates in improving the model performance (e.g., in the training round  $t$ , the cloud server randomly selects  $\mathcal{S}_n^t$  clients out of  $\mathcal{N}$ ). Besides, clients have the right to use or share their dataset  $\mathcal{D}$ , and the local loss

function of a client is defined as  $F$ . In R3T, the cloud server initiates global model parameters  $w$  and seeks high-quality clients to optimize the global model performance. It receives local model updates from clients, conducts model aggregation, and handles payments via a blockchain platform.

### B. Learning Workflow

R3T is designed to perform model training, storage, and reward calculation and allocation in a fair and auditable manner, leveraging blockchain and FL technologies. It integrates a time-aware contract theory-based mechanism to address right-time and right-reward allocation where CLPs phenomenon exists. The R3T's **one-training-round** process involves the following steps. 1) **Prepare contracts.** The cloud initiates a global model  $w$ , designs a set of contract items, and distributes them to  $N$  registered clients. 2) **Sign contracts & Download global model.** Each client signs a contract item to participate in the training process and downloads the global model  $w$ . 3) **Local training.** Clients train  $w$  using their private data  $\mathcal{D}$ . 4) **Upload updates.** Clients send their trained model updates, metadata (e.g., IDs, addresses, chosen contracts), and hashed trained model updates to their associated edge servers after training<sup>3</sup>. 5) **Forward & Validate updates.** Edges relay trained model updates to the cloud to minimize latency in the model aggregation process, and cross-validate hashed trained model updates and metadata to ensure data integrity and maintain consensus, storing records on the blockchain for transparency and dispute arbitration. 6) **Receive & Aggregate model updates<sup>4</sup>.** The cloud aggregates them using an aggregation algorithm such as FedAvg [2]. 7) **Settlement.** The process iterates until the global model converges. Upon completion, smart contracts calculate and distribute rewards to clients to compensate for their contributions (i.e., time and effort). Edge servers also receive rewards for validating transactions and storing data.

### C. Time Frame, Client Type, Contract, and Strategy

1) **Time Frame:** The time frame is divided into  $T$  training rounds<sup>5</sup>, denoted as  $\mathcal{T} = \{1, \dots, t, \dots, T\}$ , in which CLPs  $\subset \mathcal{T}$  are vital duration in determining the final model performance.

2) **Client Type:**  $N$  clients are classified into a set  $\mathcal{K} = \{1, \dots, k, \dots, K\}$  of  $K$  distinct types according to their available time and system capabilities (e.g., computation resources, and the quantity and diversity of data) due to statistical and system heterogeneity among them in real-world conditions. We denote the capability of a client  $n$  in terms of time and system resources of a type- $k$  client ( $1 \leq k \leq K$ ) by  $\theta_{n,k}$  or  $\theta_k$ <sup>6</sup>.

<sup>3</sup>We assume that clients are truthful in reporting their updates to the cloud. If required, the cloud can verify their updates using the Trusted Execution Environments [39] or reputation systems [40]. Besides, given the traceability property of the underlying blockchain [26] and incentive mechanism design (e.g., incentive compatibility) presented later in Section III, clients are encouraged to truthfully report to benefit from joining and contributing.

<sup>4</sup>To avoid the straggler effect, we employ a synchronous learning update scheme, which has a provable convergence [41], [42].

<sup>5</sup>In this work, training rounds and time slots are used interchangeably.

<sup>6</sup>For simplicity, we interchangeably represent  $\theta_{n,k}$  and  $\theta_k$  for a type- $k$  client  $n$ 's capability. Similarly, the contract item  $\phi_k$  can be denoted as  $\{e_{n,k}, t_{n,k}, R_{n,k}\}$  or  $\{e_k, t_k, R_k\}$ . The same notation applies to the model parameter  $w$ , which is introduced later.

**Definition 1.** *Without loss of generality, client training capabilities in  $K$  types belong to a discrete and finite set, as sorted in ascending order by  $0 < \theta_1 < \dots < \theta_K$ .*

It signifies that higher client types have greater training capabilities and a higher willingness to participate early, especially in CLPs, as well as be able to contribute high efforts (e.g., a huge amount of closer-distribution-to-the-learning-task data [34]). The cloud is unaware of the exact client types, knowing only the probability of a client belonging to a certain type  $k$ . Due to privacy regulations, direct collection of client-specific information is restricted, making it challenging to predict individual client capabilities. Instead, aggregate statistical insights can be obtained through market research and surveys conducted with client consent [43].

3) **Cloud's Contract:** To motivate clients to join early, share resources, and conduct training, the cloud must offer transparent and fair contribution-reward bundles, compensating clients for their efforts. Recognizing the importance of CLPs, the cloud offers extra bounties to attract high-quality, resource-rich clients to participate actively. Consequently, each client's gain is influenced by their chosen time of participation in the training process. The cloud has a contract set  $\phi = \{\phi_k\}_{k \in \mathcal{K}}$ , which contains  $K$  contract items corresponding to  $K$  client types per training round. The contract item  $\phi_k = \{e_k, t_k, R_k\}$  specifies the relationship between type- $k$  client's effort, joining time, and reward. Specifically,  $e_k$  is defined as the normalized local training effort, which can be determined jointly by the volume and the distribution of local data [34], and  $t_k$  is the training time slot, which is either in CLPs or in non-CLPs. Also,  $R_k$  is the corresponding reward for type- $k$  client paid by the cloud server for finishing the training round, and is given as follows:

$$R_k = r_k + B_k, B_k = \theta_k h(t_k) e_k, \quad (1)$$

where  $r_k$  is the basic salary and  $B_k$  is the bonus, which has been shown as an effective payment structure to motivate clients' efforts toward collective goals (i.e., enhancing global model performance) [44]. Specifically, clients are assured to have a base compensation of salary  $r$  upon joining the training process. Based on their individual types, the timing of their participation, and the level of effort they contribute, bonuses are awarded. These bonuses direct clients participating in CLPs to contribute more efforts during this period, as well as providing additional rewards for the highest-contributing clients [45]. Besides, inspired by the demand-price relationships in [46], we propose a function  $h(t_k)$  which is a time-aware bonus unit function (i.e., bonus-time relationship function), where the crucial role of CLPs is known by clients, and is presented as follows:

$$h(t_k) = \begin{cases} 1 + \frac{\vartheta}{\ln(2t_k)} & \text{if } t_k \in \text{CLPs}; \\ 1 & \text{if } t_k \in \text{non-CLPs}, \end{cases} \quad (2)$$

where  $\vartheta$  represents the bonus unit coefficient. That function offers high-quality clients bonuses when they choose to join the model training process at an early stage, given the importance of CLPs. To identify CLPs, the relative change in the weighted-average training losses aggregated over all

selected type- $k$  clients between two consecutive rounds can be monitored. If this loss reduction exceeds a pre-defined threshold, the current round is in CLPs [14].

4) *Client's Strategy Space*: Each client decides whether to participate in the training process (if yes), how much effort they should exert, and which time slot to join. The choice of different time slots may result in varying bonuses. Particularly, participating during the CLPs yields higher payoffs for clients who contribute significant effort, as training the global model with huge effort during these periods is crucial for improving final model performance.

#### D. Utilities

According to (1),  $R_k$  is dependent on  $e_k$ ,  $t_k$ , and  $r_k$ , thus each contract item is rewritten by  $\phi_k = \{e_k, t_k, r_k\}$ . We define the utilities of each client, edge server, and cloud server per training round as follows.

1) *Clients*: The utility of type- $k$  client  $n$  can be defined by:

$$\begin{aligned} \mathcal{U}_n(e_k, t_k, r_k) &= R_k - \left( \frac{1}{2} \delta e_k^2 + \beta r_k \right) \\ &= \theta_k h(t_k) e_k - \frac{1}{2} \delta e_k^2 - (\beta - 1) r_k, \end{aligned} \quad (3)$$

where  $\left( \frac{1}{2} \delta e_k^2 + \beta r_k \right)$  is the total contribution cost. This includes  $\frac{1}{2} \delta e_k^2$ , which is a quadratic cost function with respect to client's effort (e.g., sensing, collecting, and training of data or using cloud services for these tasks) according to [24], with  $\delta > 0$  being a quadratic unit effort cost that varies on different learning tasks (e.g., generating data samples or training data samples). For example, training ChatGPT-3 with 45TB of compressed plaintext before filtering and 570GB after filtering using 80 V100 GPUs costs more than \$2 million, or generating 100,000 data points using Amazon's Mechanical Turk service will cost around \$70,000 [47]. Additionally,  $\beta r_k$  represents the time cost associated with joining time  $t_k$ , considered as a linear function of the reward, where  $\beta > 1$  is the time cost coefficient [24], [48].

2) *Edge Server*: The edge server  $l$ 's utility is defined as  $\mathcal{U}_l = R_l - v(f_l)$ , where  $R_l$  is the gain from validating data transactions,  $v(f_l)$  is the validation cost function, and  $f_l$  is the edge server's computing resource (e.g., CPU-cycle frequency).

3) *Cloud server*: The cloud's utility is the difference between the gain (i.e., FL model performance) and costs (i.e., rewards for clients' contributions such as joining time and efforts in training the FL model, and for edge servers in validating data transactions) as follows:

$$\mathcal{U}_c(e, t, r) = \lambda \sum_{k \in \mathcal{K}} g(h(t_k) e_k) - \sum_{k \in \mathcal{K}} R_k - \sum_{l \in \mathcal{L}} R_l, \quad (4)$$

where  $\lambda$  is a parameter adjusted by the cloud server to show its concerns for FL model performance (i.e., larger  $\lambda$ ) or reward budget (i.e., smaller  $\lambda$ ),  $e = \{e_1, \dots, e_K\}$ ,  $t = \{t_1, \dots, t_K\}$ , and  $r = \{r_1, \dots, r_K\}$ . In each training round, multiple clients may select the same contract item  $k$ , and  $R_k$  in (4) denotes the *aggregate reward cost* incurred by the cloud for all participating clients choosing item  $k$  in that round; this aggregate notation keeps (4) compact while remaining consistent with

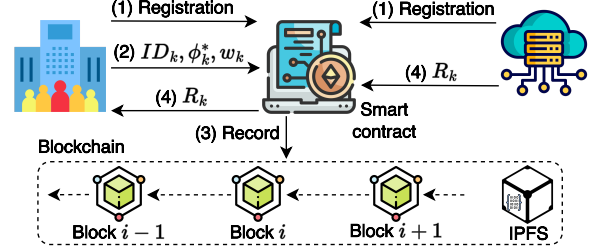


Fig. 3: Procedure of R3T based smart contracts.

the budget feasibility constraint, which is defined in the next section. Without the loss of generality,  $g(\cdot)$  is defined as a concave function [16], [49] with respect to the amount of effort and joining time. Specifically, with the same effort, each client can make different contributions and impacts on FL model performance at different training times.

#### E. Blockchain smart contract-based R3T procedure

Our focus is on the incentive mechanism design given the existence of CLPs in FL, which can be considered as a service and is built on top of the underlying blockchain [25], [26], thereby issues of blockchain security and scalability are out of scope in this article. Specifically, R3T uses smart contracts to credibly enable client and cloud registration, effort record, data storage, and reward calculation and distribution without involvement of third parties. In case of disputes between clients and the cloud, the immutably recorded results on the blockchain can serve as reliable evidence for arbitration.

Fig. 3 illustrates the functionality of blockchain and smart contracts, including four main operations. 1) First, clients and the cloud initiate their participation. During this process, R3T records information, such as IDs, and wallet addresses, for both clients and the cloud server to ensure that only registered participants can interact within the system. Additionally, the cloud publishes a contract set  $\phi^*$ , where  $\phi^*$  is a set of optimal contract items determined by the cloud in Section III, directly onto the blockchain for transparency and accessibility to clients. 2) Upon completing the training process, clients upload their strategy profiles or selected contract items  $\phi_k^*$  with their IDs, the location of the model weights, and hashed model weights to the blockchain by invoking *contributionSubmit()* function in the *Contribution* smart contract. 3) To enhance the scalability, minimize on-chain storage overhead, and provide robustness to single-point-of-failure attacks for the cloud server of R3T, *dataStore()* in the *Contribution* smart contract is employed. Global model weights are uploaded to private IPFS built by authorized edge servers while the resulting hash and corresponding training round number are recorded on-chain, ensuring data integrity and efficient and decentralized model management. 4) Finally, contract-based rewards  $R_k$  (e.g., tokens or cryptocurrencies such as Ether in the Ethereum blockchain platform) are calculated and distributed through *reward()* function in the *Reward* smart contract.

Next, we analyze R3T under two information conditions over CLPs and non-CLPs. 1) *Complete Information Case*: Clients' types are public and known to the cloud and other

clients. However, this case is impractical due to privacy leakage risks from exposing individual properties. 2) *Incomplete Information Case*: Clients' types are private and measured locally, but the cloud may statistically know the distribution of clients' types via market research or surveys [43].

### III. R<sub>3</sub>T - THE PROPOSED INCENTIVE MECHANISM FOR CRITICAL LEARNING PERIODS

#### A. Problem Formulation

A feasible contract set ensures clients, who choose their true preference types, receive equitable rewards that are commensurate with their costs and effort. Besides, in each training round, the cloud server can only afford a given budget  $P$  for rewarding. To achieve this, it must satisfy the following individual rationality (IR), incentive compatibility (IC), and budget feasibility (BF) constraints:

**Definition 2** (Individual Rationality). *Each type- $k$  client only chooses the contract item if and only if its utility is non-negative,*

$$\mathcal{U}_n(e_k, t_k, r_k) \geq 0, \forall k \in \mathcal{K}, \forall t_k \in \mathcal{T}. \quad (5)$$

**Definition 3** (Incentive Compatibility). *Each type- $k$  client maximizes its utility by choosing the contract item  $\{e_k, t_k, r_k\}$ , which is specifically designed for its type and is presented by*

$$\mathcal{U}_n(e_k, t_k, r_k) \geq \mathcal{U}_n(e_{k'}, t_{k'}, r_{k'}), \forall k, k' \in \mathcal{K}, k \neq k'. \quad (6)$$

**Assumption 1** (Rationality). *Each client is willing to join and contribute its effort to the training process, which guarantees IR and IC constraints and leads to the best utility for itself [24]. For example, realizing the importance of CLPs with a correspondingly huge amount of rewards announced by the cloud server<sup>7</sup>, each client tends to join and allocate efforts in this period.*

**Definition 4** (Budget Feasibility). *The total rewards for all participating type- $k$  clients do not exceed cloud budget  $P$ , i.e.,*

$$\sum_{k=1}^K R_k \leq P. \quad (7)$$

To maximize the utility, the cloud server offers the optimal contract set  $\phi^* = \{e^*, t^*, r^*\}$  to clients. The optimal contract set is the solution to the following problem<sup>8</sup>:

$$\max_{(\mathbf{e}, \mathbf{t}, \mathbf{r})} \mathcal{U}_c(\mathbf{e}, \mathbf{t}, \mathbf{r}), \quad (8a)$$

$$\text{s.t. } (5), (6), (7), \forall t_k \in \mathcal{T}, \forall k \in \mathcal{K}. \quad (8b)$$

Given the cloud server's contract, we model the game among clients as follows

- *Players*:  $|\mathcal{S}_n|$  clients are in the set  $\mathcal{N}$  per training round.
- *Strategies*: each client  $n \in \mathcal{S}_n$  decides which contract item  $\phi_k = \{e_k, t_k, r_k\} \in \phi$  to choose based on its capability for model training task published by the cloud server.
- *Objectives*: each type- $k$  client  $n$  aims to maximize its utility  $\mathcal{U}_n(e_k, t_k, r_k)$  expressed in (3).

<sup>7</sup>That is considered as common knowledge [24].

<sup>8</sup>The total blockchain mining rewards are constant because the computing resources required for this task are the same across all edge servers in each global training round [36]. Thus, this factor does not affect the optimization and analysis in this paper, so we omit it here.

Once  $t_k$  and  $r_k$  are given, we determine that the utility of a client in (3) is a strictly concave function with respect to its effort  $e_k$ . Hence, the optimal choice of effort  $e_k$  for a type- $k$  client can be obtained by setting the first-order derivative of the client's utility function with respect to  $e_k$ . Specifically,

$$e_k^* = \frac{\theta_k h(t_k)}{\delta}. \quad (9)$$

From (2) and (9), we can see that the optimal effort of each type- $k$  client is greater than zero and independent of  $r_k$ , but is increasing with its time and system capability  $\theta_k$  and is decreasing with joining time  $t_k$ . In other words, if a client is willing to join early and has high-system capabilities, it has a higher chance of receiving more bonuses and rewards.

Substituting  $e_k^*$  into (1), (3), (4), the utilities of a type- $k$  client and the cloud server are rewritten respectively as

$$R_k = r_k + \frac{\theta_k^2 h^2(t_k)}{\delta}, \quad (10)$$

$$\mathcal{U}_n(t_k, r_k) = \frac{\theta_k^2 h^2(t_k)}{2\delta} - (\beta - 1)r_k, \quad (11)$$

$$\mathcal{U}_c(\mathbf{t}, \mathbf{r}) = \sum_{k=1}^K \left[ \lambda g\left(\frac{\theta_k h^2(t_k)}{\delta}\right) - \left(r_k + \frac{\theta_k^2 h^2(t_k)}{\delta}\right) \right]. \quad (12)$$

The optimal contract design can be rewritten by

$$\max_{(\mathbf{t}, \mathbf{r})} \mathcal{U}_c(\mathbf{t}, \mathbf{r}), \quad (13a)$$

$$\text{s.t. } (5), (6), (7), \forall t_k \in \mathcal{T}, \forall k \in \mathcal{K}. \quad (13b)$$

#### B. R<sub>3</sub>T Incentivization under Complete Case

We study scenarios where the cloud server knows clients' time and system capabilities precisely before any interaction. This serves as an ideal benchmark, but it may be infeasible in real-world applications due to privacy regulations.

With precise knowledge of each client's type (i.e., client's available time and system capabilities), the cloud server can tailor personalized contracts to clients. Each type- $k$  client receives a corresponding contract item  $\phi_k = \{e_k, t_k, r_k\}$ , ensuring that IC and BF constraints in (6) and (7) are satisfied. The cloud server only considers the IR constraints in (5) for feasible contract design. The optimal contract design under the complete information case can be formulated as

$$\max_{(\mathbf{t}, \mathbf{r})} \sum_{k=1}^K \left[ \lambda g\left(\frac{\theta_k h^2(t_k)}{\delta}\right) - r_k - \frac{\theta_k^2 h^2(t_k)}{\delta} \right], \quad (14a)$$

$$\text{s.t. } \frac{\theta_k^2 h^2(t_k)}{2\delta} - (\beta - 1)r_k \geq 0, \quad (14b)$$

$$\sum_{k=1}^K \left[ r_k + \frac{\theta_k^2 h^2(t_k)}{\delta} \right] \leq P, \forall t_k \in \mathcal{T}, \forall k \in \mathcal{K}. \quad (14c)$$

**Theorem 1.** *All optimal contract items satisfy the condition  $\frac{\theta_k^2 h^2(t_k)}{2\delta} - (\beta - 1)r_k = 0, \forall k \in \mathcal{K}$  under the complete information case, that is the client's utility is zero.*

*Proof.* A rational cloud server aims to exploit contributions (i.e., effort and early-available time) from clients, leading to zero utility for clients. To be more specific, the cloud server always chooses a larger effort  $e_k$  (i.e., a larger  $h(t_k)$

where  $e_k = \frac{\theta_k h(t_k)}{\delta}$  shown in (9)), and a larger salary  $r_k$ . By increasing these variables, the cloud incentivizes clients to join promptly and invest time and effort in model training. In other words, the cloud exhausts its budget to quickly achieve model convergence as long as the IR constraints are not violated, specifically,  $\frac{\theta_k^2 h^2(t_k)}{2\delta} - (\beta - 1)r_k = 0$ .  $\square$

It is important to note that a larger  $h(t_k)$  means a smaller  $t_k$  that is at the early training stage. The optimal contract design in (14a) is rewritten by:

$$\max_{(\mathbf{t}, \mathbf{r})} \sum_{k=1}^K \left[ \lambda g\left(\frac{\theta_k h^2(t_k)}{\delta}\right) - r_k - \frac{\theta_k^2 h^2(t_k)}{\delta} \right], \quad (15a)$$

$$\text{s.t. } \frac{\theta_k^2 h^2(t_k)}{2\delta} - (\beta - 1)r_k = 0, \quad (15b)$$

$$\sum_{k=1}^K \left[ r_k + \frac{\theta_k^2 h^2(t_k)}{2\delta} \right] \leq P, \forall t_k \in \mathcal{T}, \forall k \in \mathcal{K}. \quad (15c)$$

In (15b), by replacing  $r_k = \frac{\theta_k^2 h^2(t_k)}{2\delta(\beta-1)}$ , we have

$$\max_{\mathbf{t}} \sum_{k=1}^K \left[ \lambda g\left(\frac{\theta_k h^2(t_k)}{\delta}\right) - \frac{\theta_k^2 h^2(t_k)}{2\delta(\beta-1)} - \frac{\theta_k^2 h^2(t_k)}{\delta} \right], \quad (16a)$$

$$\text{s.t. } \sum_{k=1}^K \left[ \frac{\theta_k^2 h^2(t_k)}{2\delta(\beta-1)} + \frac{\theta_k^2 h^2(t_k)}{\delta} \right] \leq P, \forall t_k \in \mathcal{T}, \forall k \in \mathcal{K}. \quad (16b)$$

Therefore, by utilizing exhaustive search, we can calculate optimal values of  $h(t_k)$  and  $t_k$ , then  $r_k$ ,  $R_k$ , and  $e_k$ .

### C. R3T Incentivization under Incomplete Information Case

We now introduce the contract game in an incomplete information setting. Clients choose contract items (i.e., effort, joining time, and corresponding reward) offered by the cloud. While the cloud aims to optimize its utility (e.g., global model performance), clients seek to maximize their incentives.

**Lemma 1** (Monotonicity in CLPs). *The higher-type client should receive a higher reward  $R$  when they join the training process early and contribute more effort. Otherwise, all clients would opt for higher-type contract items but join later and contribute less effort. Thus, under the IC constraints, if  $\theta_k > \theta_{k'}$ ,  $\forall k, k' \in \mathcal{K}$ , then the reward (including salary and bonus), effort, and joining time satisfy the following inequalities:*

$$R_k > R_{k'}, r_k \geq r_{k'}, B_k > B_{k'}, e_k > e_{k'}, t_k \leq t_{k'}. \quad (17)$$

*Proof.* According to the IC constraints in (6), we have

$$\frac{\theta_k^2 h^2(t_k)}{2\delta} - (\beta - 1)r_k \geq \frac{\theta_{k'}^2 h^2(t_{k'})}{2\delta} - (\beta - 1)r_{k'}, \quad (18)$$

$$\frac{\theta_{k'}^2 h^2(t_{k'})}{2\delta} - (\beta - 1)r_{k'} \geq \frac{\theta_k^2 h^2(t_k)}{2\delta} - (\beta - 1)r_k, \quad (19)$$

with  $k, k' \in \mathcal{K}, k \neq k'$ . Summing up (18) and (19), we obtain

$$\frac{h^2(t_k)}{2\delta}(\theta_k^2 - \theta_{k'}^2) \geq \frac{h^2(t_{k'})}{2\delta}(\theta_k^2 - \theta_{k'}^2). \quad (20)$$

As  $\theta_k > \theta_{k'} > 0$ , we have  $(\theta_k^2 - \theta_{k'}^2) > 0$ . Dividing both sides by  $(\theta_k^2 - \theta_{k'}^2)$ , we have  $h^2(t_k) \geq h^2(t_{k'})$  and as  $h(t_k) \geq$

$1, \forall k \in \mathcal{K}$ , we conclude  $h(t_k) \geq h(t_{k'})$ . In addition, because  $h(t_k)$  is a strictly decreasing function of  $t_k$ , we can obtain  $t_k \leq t_{k'}$ . Also, we prove if  $h(t_k) \geq h(t_{k'})$ , then  $r_k \geq r_{k'}$  under the IC constraints. Based on (19), we have

$$\begin{aligned} (\beta - 1)r_k - (\beta - 1)r_{k'} &\geq \frac{\theta_{k'}^2 h^2(t_k)}{2\delta} - \frac{\theta_k^2 h^2(t_{k'})}{2\delta}, \\ (\beta - 1)(r_k - r_{k'}) &\geq \frac{\theta_{k'}^2}{2\delta} [h^2(t_k) - h^2(t_{k'})] \geq 0. \end{aligned} \quad (21)$$

Since  $\beta > 1$  and  $h(t_k) \geq h(t_{k'})$ , thus  $r_k \geq r_{k'}$ . Next, with the conditions of  $\theta_k > \theta_{k'}$ ,  $h(t_k) \geq h(t_{k'})$ , and (9), we have  $e_k > e_{k'}$ . As a result, we conclude  $B_k > B_{k'}$ , thereby  $R_k > R_{k'}$  based on (1). This completes the proof.  $\square$

**Lemma 2** (Client utility condition). *For any feasible contract item  $(e_k, t_k, r_k)$ , the type- $k$  client's utility satisfies*

$$\begin{aligned} \mathcal{U}_n(e_1, t_1, r_1) &< \dots < \mathcal{U}_n(e_k, t_k, r_k) < \dots \\ &< \mathcal{U}_n(e_K, t_K, r_K). \end{aligned} \quad (22)$$

*Proof.* According to Lemma 1, high-type clients who receive more rewards must contribute greater efforts and join as early as possible (i.e.,  $R_k > R_{k'}$ ,  $e_k > e_{k'}$  and  $t_k \leq t_{k'}$  are imposed together). Upon the conditions that  $\theta_k > \theta_{k'}$  and (9), we have

$$\begin{aligned} \mathcal{U}_n(e_k, t_k, r_k) &= \frac{\theta_k^2 h^2(t_k)}{2\delta} - (\beta - 1)r_k \geq \frac{\theta_{k'}^2 h^2(t_{k'})}{2\delta} - (\beta - 1)r_{k'} \\ &> \frac{\theta_{k'}^2 h^2(t_{k'})}{2\delta} - (\beta - 1)r_{k'} = \mathcal{U}_n(e_{k'}, t_{k'}, r_{k'}). \end{aligned} \quad (23)$$

This completes the proof.  $\square$

**Lemma 3** (Simplify the IR constraints). *In the optimal contract, given that IC constraints in (6) are satisfied, the IR constraint for type-1 client is binding, i.e.,  $\frac{\theta_1^2 h^2(t_1)}{2\delta} - (\beta - 1)r_1 = 0$ .*

*Proof.* According to Lemma (2), we have

$$\frac{\theta_k^2 h^2(t_k)}{2\delta} - (\beta - 1)r_k \geq \frac{\theta_1^2 h^2(t_1)}{2\delta} - (\beta - 1)r_1 \geq 0. \quad (24)$$

As such, if the IR constraint of type-1 client is binding, that of all other types holds. This completes the proof.  $\square$

The IR constraints in (5) can be replaced by Lemma (3), which indicates that this type-1 client gains or loses nothing in participating in training, while other client's utilities are higher than that of the binding one. Next, we refer to [50] to introduce the following definitions for simplifying IC constraints:

**Definition 5** (Conditions for IC constraints). 1) *Downward incentive constraints (DICs) are IC constraints between client types  $k$  and  $k'$ , where  $1 \leq k' \leq k - 1$ , 2) local downward incentive constraints (LDIC) is an IC constraint between client's types  $k$  and  $k'$ , where  $k' = k - 1$ , 3) upward incentive constraints (UICs) are IC constraints between client's types  $k$  and  $k'$ , where  $k + 1 \leq k' \leq K$ , and 4) local upward incentive constraints (LUIC) is an IC constraint between client's types  $k$  and  $k'$ , where  $k' = k + 1$ .*

**Lemma 4** (Simplify the IC constraints). *In the optimal contract, we can replace the IC constraints in (6) by*

$$\frac{\theta_k^2 h^2(t_k)}{2\delta} - (\beta - 1)r_k = \frac{\theta_{k-1}^2 h^2(t_{k-1})}{2\delta} - (\beta - 1)r_{k-1}. \quad (25)$$

*Proof.* We consider three client types where  $\theta_{k-1} < \theta_k < \theta_{k+1}, \forall k \in \mathcal{K}$ . Under IC constraints, we have two LDICs

inequalities as follows

$$\frac{\theta_{k+1}^2 h^2(t_{k+1})}{2\delta} - (\beta - 1)r_{k+1} \geq \frac{\theta_{k+1}^2 h^2(t_k)}{2\delta} - (\beta - 1)r_k, \quad (26)$$

$$\frac{\theta_k^2 h^2(t_k)}{2\delta} - (\beta - 1)r_k \geq \frac{\theta_k^2 h^2(t_{k-1})}{2\delta} - (\beta - 1)r_{k-1}. \quad (27)$$

By virtue of monotonicity in Lemma 1, the condition of  $\theta$ , and (27), we have

$$\begin{aligned} \frac{\theta_{k+1}^2}{2\delta} [h^2(t_k) - h^2(t_{k-1})] &\geq \frac{\theta_k^2}{2\delta} [h^2(t_k) - h^2(t_{k-1})] \\ &\geq (\beta - 1)(r_k - r_{k-1}). \end{aligned} \quad (28)$$

As a result, we convert (26) as

$$\begin{aligned} \frac{\theta_{k+1}^2 h^2(t_{k+1})}{2\delta} - (\beta - 1)r_{k+1} &\geq \frac{\theta_{k+1}^2 h^2(t_k)}{2\delta} - (\beta - 1)r_k \\ &\geq \frac{\theta_{k+1}^2 h^2(t_{k-1})}{2\delta} - (\beta - 1)r_{k-1}. \end{aligned} \quad (29)$$

Therefore, we conclude that LDIC has transitivity, i.e., if there is an LDIC between type- $(k-1)$  and type- $k$  clients, then we can further extend incentive constraints from type- $(k-1)$  client to type-1 client, that is, all DICs hold, i.e.,

$$\begin{aligned} \frac{\theta_{k+1}^2 h^2(t_{k+1})}{2\delta} - (\beta - 1)r_{k+1} &\geq \frac{\theta_{k+1}^2 h^2(t_k)}{2\delta} - (\beta - 1)r_k \\ &\geq \frac{\theta_{k+1}^2 h^2(t_{k-1})}{2\delta} - (\beta - 1)r_{k-1} \\ &\geq \dots \\ &\geq \frac{\theta_{k+1}^2 h^2(t_1)}{2\delta} - (\beta - 1)r_1. \end{aligned} \quad (30)$$

Thus, we have proved that with the LDIC, all DICs hold. Similarly, with the LUIC, all UICs are satisfied. We can write a generalization of DICs and UICs, respectively, as follows

$$\begin{aligned} \frac{\theta_k^2 h^2(t_k)}{2\delta} - (\beta - 1)r_k &\geq \frac{\theta_{k'}^2 h^2(t_{k'})}{2\delta} - (\beta - 1)r_{k'}, \\ 1 \leq k' < k \leq K, \\ \frac{\theta_k^2 h^2(t_k)}{2\delta} - (\beta - 1)r_k &\geq \frac{\theta_{k'}^2 h^2(t_{k'})}{2\delta} - (\beta - 1)r_{k'}, \\ 1 \leq k < k' \leq K. \end{aligned} \quad (31)$$

Therefore, the IC constraints are reduced to

$$\frac{\theta_k^2 h^2(t_k)}{2\delta} - (\beta - 1)r_k \geq \frac{\theta_{k-1}^2 h^2(t_{k-1})}{2\delta} - (\beta - 1)r_{k-1}, \quad (32)$$

which replace IC constraints in (6). This completes proof.  $\square$

**Theorem 2.** For any type- $k$  client, the contract salary satisfies

$$r_k = \sum_{i=1}^k \frac{\theta_i^2 [h^2(t_i) - h^2(t_{i-1})]}{2\delta(\beta - 1)}.$$

*Proof.* Based on Lemma 3, the salary of type-1 client can be calculated as follows

$$r_1 = \frac{\theta_1^2 h^2(t_1)}{2\delta(\beta - 1)}. \quad (33)$$

---

### Algorithm 1: Game and Training Process of R3T

---

**Input:** A set of clients  $\mathcal{N}$ , number of training rounds  $T$ , learning rate  $\eta$ , local loss function  $F$ , initial global parameter  $w^0$ , bonus unit coefficient  $\vartheta$ .  
**Output:** Final global model parameter  $w^T$ .  
**Data:** Training, validation, and test set  $\mathcal{D}$ .

```

1 for  $t = 1, 2, \dots, T$  do
2   > Cloud performs:
3   Obtain an optimal contract set  $\phi^*$  via (16) or (36).
4   Send the set  $\phi^* = \{e^*, t^*, r^*\} = \{\phi_k^*\}_{k \in \mathcal{K}}$  to  $\mathcal{N}$ .
5   Select a client subset  $S_n^t$  from  $\mathcal{N}$ .
6   > Clients perform:
7   for each client  $n \in S_n^t$  in parallel do
8     Sign contract items  $\{\phi_k^*\}_{k \in \mathcal{K}}$ .
9     if  $t_k^* = t$  then
10      Download  $w^{t-1}$ .
11      Adjust  $\mathcal{D}_k$  according to  $e_k^*$ .
12       $w_k^t \leftarrow w_k^{t-1} - \eta \nabla F_k(w_k^{t-1}, \mathcal{D}_k)$ 
13   > Blockchain performs:
14   Cross-validate and record  $\{ID_k, \text{hash}(w_k^t), \phi_k^*\}$ .
15   > Cloud performs:
16   if  $t \in CLPs$  then
17      $|S_n^{t+1}| \leftarrow \min\{2|S_n^t|, N\}$ 
18      $h(t_k^*) = h(t) = 1 + \frac{\vartheta}{\ln(2t)}$ 
19   else
20      $|S_n^{t+1}| \leftarrow \max\{\frac{1}{2}|S_n^t|, \frac{1}{2}N\}$ 
21      $h(t_k^*) = 1$ 
22    $w^t \leftarrow \sum_{k \in \mathcal{K}} \frac{e_k^*}{\sum_{k \in \mathcal{K}} e_k^*} w_k^t$ 
23   > Blockchain performs:
24   Record  $\{h(t_k^*), w^t\}$ .
25 > Blockchain performs:
26 Calculate and allocate  $R_k^*$  to type- $k$  clients via (1).
27 Return  $w^T$ .

```

---

Then, according to Lemma 4 and (33), we can further derive

$$r_2 = r_1 + \frac{\theta_2^2 [h^2(t_2) - h^2(t_1)]}{2\delta(\beta - 1)}. \quad (34)$$

By iterating these steps, we can obtain

$$\begin{aligned} r_k &= r_{k-1} + \frac{\theta_k^2 [h^2(t_k) - h^2(t_{k-1})]}{2\delta(\beta - 1)} \\ &= \frac{\theta_k^2 [h^2(t_k) - h^2(t_{k-1})]}{2\delta(\beta - 1)} + \dots + \frac{\theta_1^2 h^2(t_1)}{2\delta(\beta - 1)} \\ &= \sum_{i=1}^k \frac{\theta_i^2 [h^2(t_i) - h^2(t_{i-1})]}{2\delta(\beta - 1)}. \end{aligned} \quad (35)$$

At  $i = 1$ , we have  $h(t_0) = 0$  because  $t_0$  is the time before the training process starts. This completes the proof.  $\square$

By using the simplified constraints above and substituting  $e_k$  and  $r_k$  with  $h(t_k)$ , the final form of the optimization problem is as follows

$$\begin{aligned} \max_t \quad & \sum_{k=1}^K \left[ \lambda g\left(\frac{\theta_k h^2(t_k)}{\delta}\right) - \sum_{i=1}^k \frac{\theta_i^2 [h^2(t_i) - h^2(t_{i-1})]}{2\delta(\beta - 1)} \right. \\ & \left. - \frac{\theta_k^2 h^2(t_k)}{\delta} \right], \end{aligned} \quad (36a)$$

$$\text{s.t.} \quad \sum_{k=1}^K \left[ \sum_{i=1}^k \frac{\theta_i^2 [h^2(t_i) - h^2(t_{i-1})]}{2\delta(\beta - 1)} + \frac{\theta_k^2 h^2(t_k)}{\delta} \right] \leq P, \quad (36b)$$

$$(17), \forall t_k \in \mathcal{T}, \forall k \in \mathcal{K}. \quad (36c)$$

TABLE I: Experimental Parameters

Param	Value	Param	Value	Param	Value
$\lambda_{\text{CLPs}}$	21	$\lambda_{\text{non-CLPs}}$	20	$\theta_k$	$U(1, 2)$
$T$	25	$N$	15	$K$	10
$C$	2.4	$\beta$	3	$t_{\text{non-CLPs}}$	$[11, T]$

Using an exhaustive search algorithm, we obtain the optimal  $t_k$  and  $h(t_k)$ , then  $r_k$  and  $R_k$ , and finally  $e_k$  without considering the monotonicity condition in (17). Then, we check if the solution satisfies the monotonicity condition in (17).

Based on the analyses and proofs above, we now analyze monotonicity conditions in the non-CLPs.

**Lemma 5** (Monotonicity in non-CLPs). *In the non-CLPs, R3T still ensures incentive fairness by enabling a higher-type client to receive a higher reward. Thus, to satisfy the IC constraints in (6), if  $\theta_k > \theta_{k'}, \forall k, k' \in \mathcal{K}$ , then the reward, salary, and effort must adhere to the following inequalities:*

$$R_k > R_{k'}, r_k = r_{k'}, e_k > e_{k'}. \quad (37)$$

*Proof.* According to (1),  $h(t_k) = 1$  and the impact of efforts in non-CLPs is not of importance as CLPs, thereby  $h(t_{k'}) = h(t_k) = 1, \forall t_k, t_{k'} \notin \text{CLPs}$ . This leads to  $e_k > e_{k'}$  based on (9). Moreover, via (35) and  $h(t_{k'}) = h(t_k)$ , we can conclude that  $r_k = r_{k'} = r_1 = \frac{\theta_k^2 h^2(t_1)}{2\delta(\beta-1)}$ . Next, with the proved conditions (i.e.,  $h(t_k) = h(t_{k'})$  and  $r_k = r_{k'}$ ), and the expression (1), we have  $R_k > R_{k'}$ . This completes the proof.  $\square$

**Remark 1.** *In non-CLPs, the impact of the client's contribution is less significant compared to CLPs. As Lemma 5 outlines, although all clients receive a fixed salary regardless of their types and do not receive weighted bonuses (i.e.,  $h(t_k) = 1$ ) for specific joining times, R3T ensures the fairness of their total rewards relative to their corresponding efforts.*

**Remark 2.** *R3T handles the information asymmetry between clients and the cloud server via a self-revelation principle by designing a menu of contract items to incentivize clients to disclose their private properties and an incentive compatibility constraint to encourage clients to truthfully choose and report their type-aligned contract items to get the best utilities. R3T guarantees the fairness in incentive distribution in both CLPs and non-CLPs as shown in Lemma 1 and Lemma 5.*

The R3T's game and training processes in  $T$  training rounds are depicted in Algorithm 1. We have a tuple of  $(e_k^*, t_k^*, r_k^*)$  being the optimal strategy of the type- $k$  client (line 3). CLPs can be identified by using federated gradient norm metric (line 16) [14]. To address the issue of insufficient client participation and its detrimental effect on final model performance, R3T increases the number of clients during the early training phase (line 17) by offering an attractive contract set. Besides, to reduce communication overhead and budget exhaustion, R3T decreases the number of clients in non-CLPs (line 20).

#### IV. EXPERIMENTAL RESULTS

In this section, we conduct extensive experiments to analyze the feasibility and efficiency of R3T. Then, we evaluate R3T's proof of concept on prominent benchmark datasets.

#### A. Experiment Setup

**Simulation parameter settings.** Without loss of generality, our experimental settings refer to the setups in [21], [51]. We also define the function  $g(\cdot)$  by  $g(\cdot) = h(t)e$ . The key parameters used in the simulations are shown in Table I.

**Proof of concept.** We develop a system to implement a proof of concept of R3T, leveraging smart contracts on an Ethereum blockchain using Ganache [52]. The Flower framework [53] is integrated with the blockchain to facilitate federated learning experiments for model training and evaluation. The system is deployed on an Ubuntu 22.04 system equipped with an Intel Core i7-1365U CPU@1.80 GHz and 32GB of memory. To enable interaction between clients, the cloud server, and the smart contracts, we utilize the Web3 API [54] and FastAPI frameworks [55]. Also, we develop two smart contracts for federated training and storage, and reward calculation using Solidity programming language.

**Model and Datasets:** We use a deep neural network with four layers comprising three convolutional neural layers with dropout to prevent overfitting, batch normalization, and max pooling for reducing spatial dimensions, and one dense layer. For model training and testing, CIFAR-10 [56] and Fashion-MNIST [57] datasets are used in a non-independent and identically distributed (non-IID) setting. We consider a highly heterogeneous setting in which the number of data samples and data labels among clients are unbalanced by sampling  $p \sim \text{Dir}(\alpha)$ , where  $\alpha = \{0.1, 0.4, 0.7\}$  is the parameter of Dirichlet distribution. Besides, the learning rate  $\eta$  is 3e-4 and the batch size is 32.

**Benchmarks.** We consider the following benchmarks in CLPs and non-CLPs for comparison with our proposed methods, which are labeled as R3T in Complete Information Case (R3T-CIC) and R3T in Incomplete Information Case (R3T-IIC).

- **Contract theory Without considering Time under CIC (CTWT-CIC).** Time property is not considered in the existing work (e.g., [21], [23], [25], [50]), that is,  $t$  is excluded from the contract item. All training time slots are treated equally.
- **Contract theory Without considering Time under IIC (CTWT-IIC).** Similar to CTWT-CIC, this method does not consider temporal importance. In addition, the cloud server only knows the distribution of clients' types.
- **Linear Pricing.** Under IIC, the cloud server determines a unit price  $C$  for the client's effort  $e$  [24].
- **Conventional Federated Learning (CFL).** FL methods integrating conventional incentive mechanisms (e.g., [23], [25], [33]), which do not consider CLPs, are used to compare with R3T proof of concept.

#### B. Contract Feasibility

We first examine the impacts of varying unit effort cost  $\delta$  and cloud budget  $P$  on R3T over  $N = 10$  clients in R3T during the initial training round of CLPs. Then, we evaluate cloud utility, effort, reward, and client utility against contract items (i.e., client types) in R3T during the initial training round of CLPs and non-CLPs starting at  $t = 1$  and  $t = 11$ ,

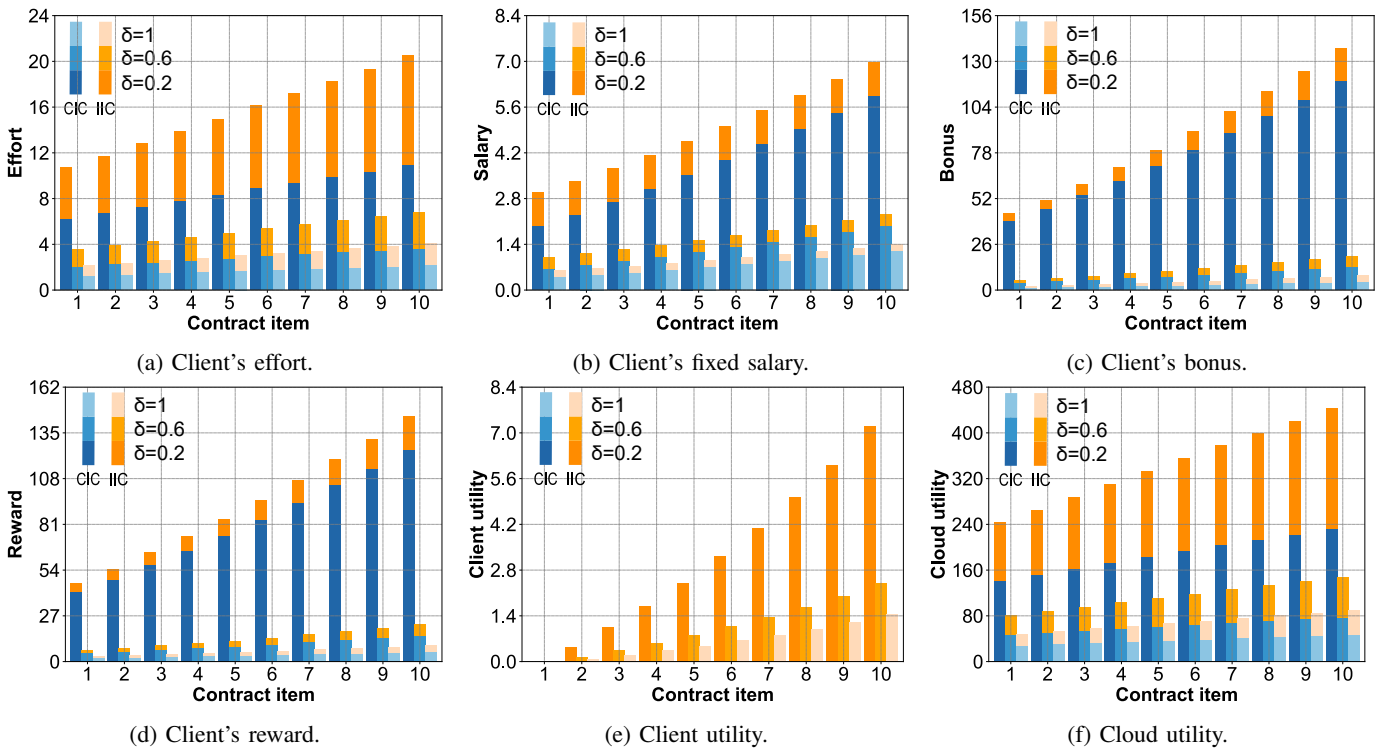


Fig. 4: The impact of unit effort cost  $\delta$  on the client’s effort, fixed salary, bonus, total reward, client utility, and cloud utility.

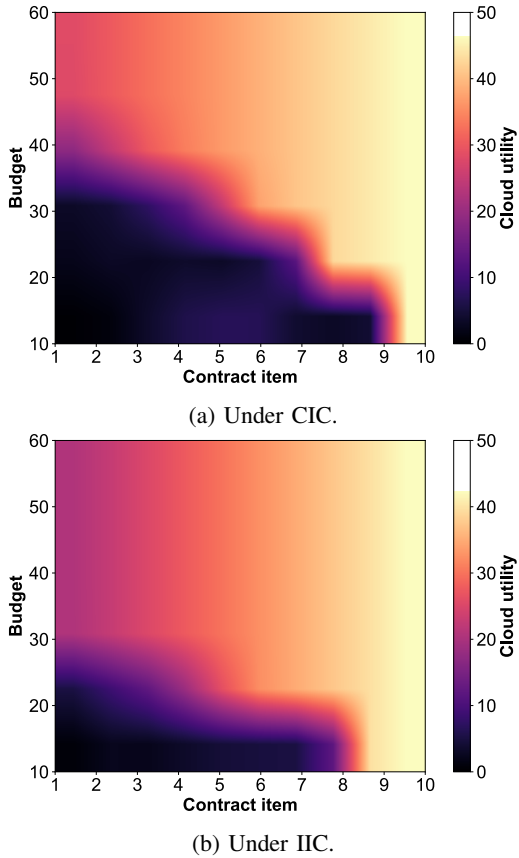


Fig. 5: The impact of cloud budget  $P$  on cloud utility per contract item and total cloud utility.

correspondingly, where we set the cloud budget  $P = 60$  per

round and  $\delta = 1$ .

**Impacts of different unit effort costs.** In Figs. 4(a)-(f), under CIC and IIC in CLPs<sup>9</sup>, the client’s fixed salary, bonus, effort, total reward, utility, and cloud utility have shown decreasing trends per contract item along with the increase of unit effort cost  $\delta$ , where we set  $\delta = \{0.2, 0.6, 1\}$ . In other words, clients are not willing to join and contribute efforts when  $\delta$  becomes large. For example, given the tenth contract item under the IIC cases, the values of the client’s effort units are around  $\{9.60, 3.20, 1.92\}$  corresponding to  $\delta = \{0.2, 0.6, 1\}$ . Besides, under CIC, where the cloud server possesses complete client information, the cloud can fine-tune and optimize its contract items to incentivize clients to join early and contribute more effort. This results in higher cloud utility while offering clients higher fixed salaries and bonuses, compared to IIC (e.g., 232.28 vs. 211.13, 5.96 vs. 1.01, and 119.21 vs. 18.47 given the tenth contract item with  $\delta = 0.2$ , respectively). In addition, due to being aware of client information, the cloud server exploits the client’s efforts as much as possible while guaranteeing IR constraints (cf. Theorem 1) in CIC, leading client utilities over contract items equal to zero (cf., Fig. 4(e)).

**Impacts of different cloud budgets.** Figs. 5(a)-(b) show the effect of varying cloud budgets  $P$  on the cloud utility contributed by type- $k$  clients (i.e.,  $k$ -th contract items) in a global training round under both CIC and IIC in CLPs. As  $P$  increases, more clients can be incentivized to participate in and allocate efforts, resulting in greater total cloud utility over all joined clients. For instance, at  $P = 60$ , the total cloud utility

<sup>9</sup>We focus on one global training round in CLPs here, but analogous trends observed in non-CLPs.

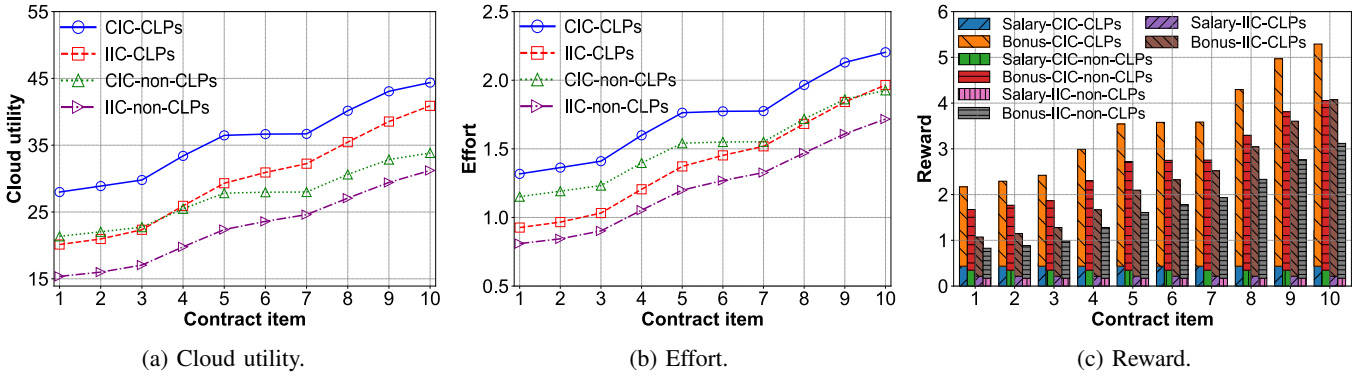


Fig. 6: Performance evaluation of R3T per training round.

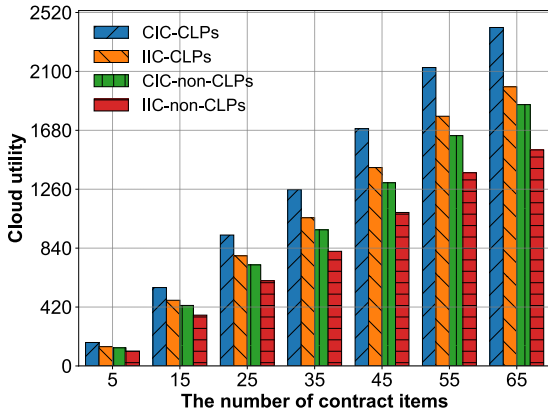


Fig. 7: Cloud utility with different number of contract items.

of all type- $k$  clients reaches approximately 375 in CIC and 312 in IIC, compared to 266 in CIC and 311 in IIC at  $P = 30$ , respectively. Especially at low budgets (i.e.,  $P = \{10, 20, 30\}$ ), the total cloud utility under IIC exceeds that under CIC. This is supported by Assumption 1 and the fact that the cloud server is aware of clients' types in CIC and only the distribution of clients' types in IIC, thereby different optimal contract designs. Consequently, in CIC, the cloud server may adopt a greedy allocation strategy to exhaust efforts from higher-type clients (cf. Theorem 1), but due to a limited budget, it leads to fewer participating clients and thus lower total cloud utility compared with that of IIC. Conversely, when the budget is huge enough (i.e.,  $P \geq 40$ ), the total cloud utility in CIC is far larger than that in IIC (i.e., 375 versus 311 at  $P = 60$ ).

**Performance evaluation.** We consider cloud utility, client's effort, and client's reward according to contract items in a training round in CLPs and non-CLPs under conditions of CIC and IIC as shown in Figs. 6(a)-(c). In Fig. 6(a), the cloud server achieves the maximum utilities in both CLPs and non-CLPs in CIC compared to IIC. This outcome occurs because the cloud server has complete knowledge of the client's capabilities, enabling it to fully leverage clients' effort and time without breaching IR constraints, thereby maximizing utility as per Theorem 1. Conversely, under IIC, the cloud server does not obtain complete information but only distribution of the client's type; therefore the cloud server's utility remains constrained by the utility attainable under CIC. Figs. 6(b)-(c) contrast efforts and rewards (comprising of salaries and

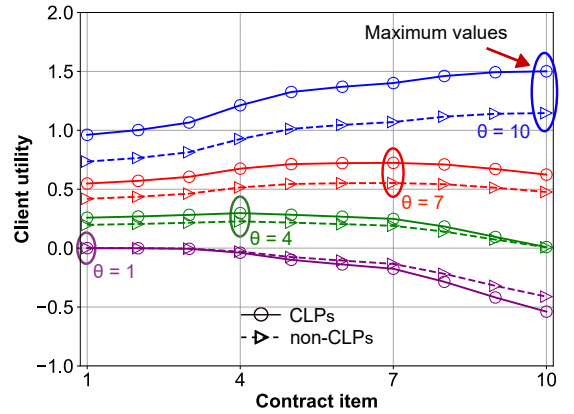
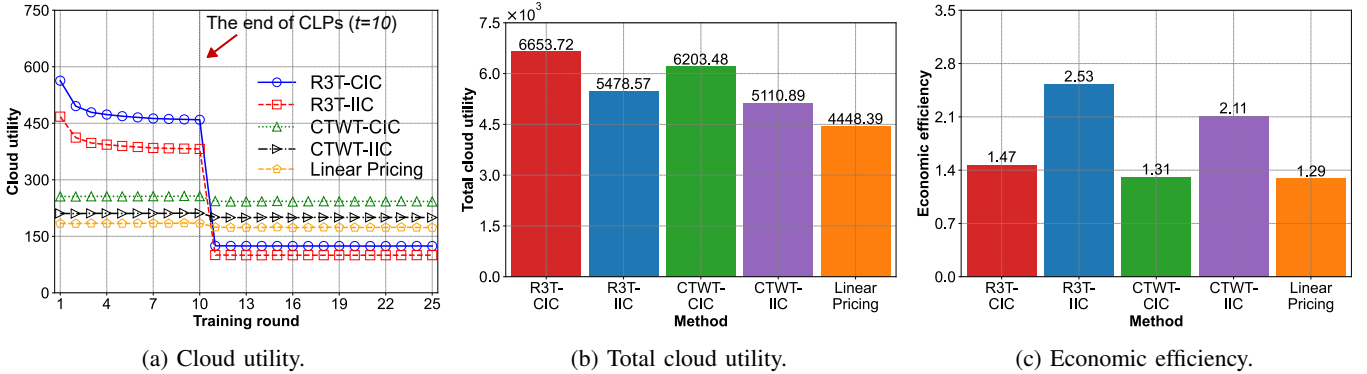
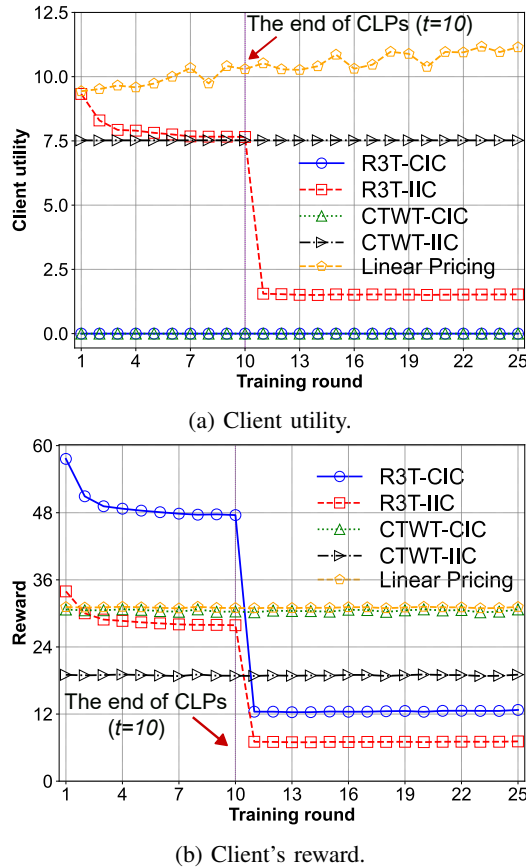


Fig. 8: Client utility under different contract items.

bonuses) associated with different contract items. These results validate the monotonicity conditions, which are detailed in Lemma 1 and Lemma 5, and Remark 1. As can be seen from the figures, higher-type clients contribute more effort and, consequently, receive higher rewards.

**Scalability.** In Fig. 7, we study the influence of the number of contract items among clients on the cloud utility. As the number of contract items increases, the cloud server can enhance its utility by enabling and motivating more higher-type clients to participate early and contribute more effort. R3T shows its scalability in diverse and expansive training environments (e.g., Internet of Things). However, expanding the number of contract items also presents a challenge of budget constraints for the cloud server.

**Contract feasibility.** In Fig. 8, the utilities of four client types are compared when they select the same contract item. Their utilities follow the inequality  $U_1 < U_4 < U_7 < U_{10}$  and each client can achieve maximum utility if and only if they select the contract item designed for their types, corroborating the results presented in Lemma 2 and Lemma 1, respectively, which explain the IC constraint. This contract design ensures that clients' types are automatically disclosed to the cloud server upon contract selection, effectively addressing information asymmetry between clients and the cloud server. Furthermore, clients receive non-negative utilities when they choose the corresponding contract items with their types, which validates the IR constraint.

Fig. 9: Cloud gain over  $T$  training rounds.Fig. 10: Client gain over  $T$  training rounds.

### C. Contract Efficiency

Fig. 9 and Fig. 10 examine the efficiency of R3T with CTWT and linear pricing with the same cloud budget  $P = 60$ , where the number of clients is  $N = 15$  and unit effort cost  $\delta = 1$ . In this comparison, we assume that CLPs span from  $t = 1$  to  $t = 10$ , and non-CLPs begin from  $t = 11$  to the end.

**Cloud utility.** Fig. 9(a) shows cloud utilities in the CLPs and non-CLPs. R3T demonstrably outperforms other methods by effectively attracting the highest-quality contributions in the CLPs. Consequently, the cloud server maintains a significantly higher utility level compared with other approaches during the CLPs, which determine the final model performance. Although the cloud utility of R3T shows a gradual decrease, which becomes more pronounced once the learning and

training process transitions to the non-CLPs (i.e.,  $t \geq 11$ ), the total R3T's cloud utility still achieves higher results in comparison with conventional incentive benchmarks, as shown in Fig. 9(b). For example, R3T showcases cloud utility up to approximately 7.2% and 23.1% higher in the IIC compared to CTWT-IIC and linear pricing methods, respectively.

Moreover, R3T demonstrates higher economic efficiency compared to conventional benchmarks, as shown in Fig. 9(c). *Economic efficiency reflects the effectiveness of the cloud server in calculating and distributing the total amount of reward to clients based on their efforts and joining times.* For instance, R3T spends approximately 20% and 96% less on the amount of reward compared with CTWT and linear pricing, respectively, while still reaching higher final cloud utility in the IIC setting. *This highlights the importance of providing the right reward at the right time.*

**Client gain.** As the importance of training rounds diminishes in non-CLPs, client utilities trend downward in R3T, as shown in Fig. 10(a). Meanwhile, the CTWT methods, which treat training rounds equally and randomly select a number of clients per round without early participation incentives, maintain stable client utilities - roughly 7.5 in CTWT-IIC methods and 0 in CTWT-CIC methods as indicated in Theorem 1 throughout the  $T$  training rounds. The linear pricing method exhibits the lowest cloud utility but the highest client utility due to its fixed price per unit of client effort. This fixed pricing approach limits information gathering for the cloud and prevents optimal price and reward adjustments to match varying client capabilities, efforts, and costs.

Fig. 10(b) shows the total client's rewards offered in  $T$  training rounds. While R3T allocates a significant amount of rewards to attract high-quality clients during the CLPs, the amount of rewards of other benchmarks remains generally stable in every training round. This again stems from the strategic allocation of rewards, prioritizing efforts made earlier in the training process in R3T, and further explaining the economic efficiency of the cloud server.

### D. Proof of Concept of R3T

In Fig. 11, we introduce a proof of concept of R3T. Clients with higher IDs are assigned higher training capabilities, characterized by larger data sizes and increased data diversity. We assume all clients have identical system capabilities and

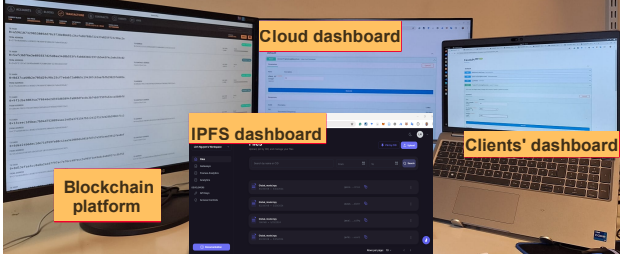
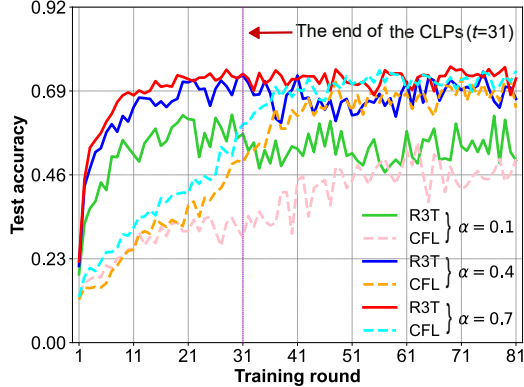
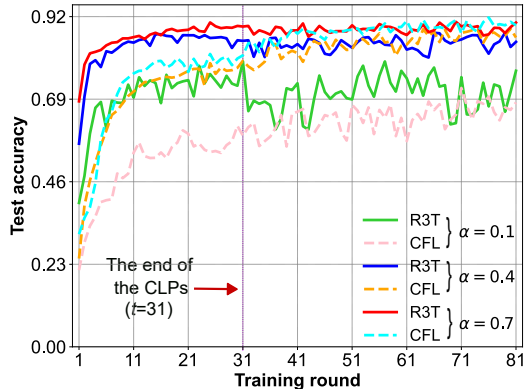


Fig. 11: R3T’s proof of concept. The system includes the Ethereum blockchain, online IPFS storage to address scalability issues, a cloud dashboard and ten clients’ dashboards.



(a) CIFAR-10.



(b) Fashion-MNIST.

Fig. 12: Test accuracy of R3T and CFL.

act rationally and strategically under Assumption 1. Besides, CLPs end at training round 31. Clients register on the blockchain and their information (e.g., IDs, addresses, efforts, and joined training rounds) is recorded throughout the training. Therefore, non-repudiation and transparency are guaranteed thanks to blockchain properties.

**Convergence rate.** As illustrated in Fig. 12, R3T demonstrates its efficiency by surpassing CFL in *improving convergence rate* under non-IID settings for both CIFAR-10 and Fashion-MNIST datasets. Particularly, R3T achieves a significant increase in performance during the initial FL training phase. This improvement is attributed to its strategy of attracting the highest-quality clients by offering an optimal set of contract items, which includes timely and substantial rewards, early in the training process. For example, R3T tends to reach the final target accuracy in just 20 rounds, compared

with approximately 61 rounds for CFL on the datasets.

**Long-term performance.** For different values of the parameter of Dirichlet distribution  $\alpha = \{0.4, 0.7\}$  in both datasets, both R3T and CFL maintain stable test accuracies after convergence, even though R3T selects a smaller number of participating clients (cf., in line 20 of Algorithm 1). Under a highly non-IID setting (i.e.,  $\alpha = 0.1$ ), R3T demonstrates *more sustainable performance* compared to CFL. In CFL, the practice of treating clients’ contributions and efforts equally across all training rounds, especially under a significant quantity and label distribution skew, detrimentally affects the long-term performance of the FL model, regardless of subsequent efforts. Besides, although R3T shows a slight drop in accuracy after CLPs due to the reduced number of selected clients, the overall test accuracy remains stable around the highest bound. These observations highlight the significant impact of attracting high-quality clients early, saving around 200%-300% in the total training time and 5.2%-47.6% in the total number of clients to achieve a close targeted learning performance.

## V. CONCLUSION

In this work, we studied R3T, a time-aware incentive framework for FL implemented on smart contracts. By characterizing the interactions between the client time and system capabilities, efforts, joining time, and their impact on cloud utility, we proposed a contract design that incorporates the temporal factor to derive optimal incentive strategies for the cloud. R3T transparently allocates the right reward at the right time, effectively attracting the highest-quality contributions during the early training phase, which is a critical determinant of final model performance under information symmetry and asymmetry. Simulation and proof-of-concept experimental results demonstrate the superiority of R3T over incentive benchmark mechanisms in cloud utility and economic efficiency. Furthermore, R3T reduces convergence time and the requisite number of participating clients, while achieving comparable model performance.

## REFERENCES

- [1] T. L. Nguyen and Q.-V. Pham, “A critical learning period-aware incentive mechanism for federated learning,” in *IEEE 101st Vehicular Technology Conference (VTC2025-Spring)*, 2025, pp. 1–6.
- [2] B. McMahan, E. Moore, D. Ramage, S. Hampson, and B. A. y Arcas, “Communication-efficient learning of deep networks from decentralized data,” in *Artificial Intelligence and Statistics*, 2017, pp. 1273–1282.
- [3] T.-B. Nguyen, M.-D. Nguyen, J. Park, Q.-V. Pham, and W. J. Hwang, “Federated domain generalization with data-free on-server gradient matching,” in *International Conference on Learning Representations (ICLR)*, May 2025.
- [4] G. Yan, H. Wang, and J. Li, “Seizing critical learning periods in federated learning,” in *Proceedings of the AAAI Conference on Artificial Intelligence*, vol. 36, 2022, pp. 8788–8796.
- [5] C. Huang and B. Liu, “Pa3fed: Period-aware adaptive aggregation for improved federated learning,” in *Proceedings of the AAAI Conference on Artificial Intelligence*, vol. 39, no. 16, 2025, pp. 17395–17403.
- [6] E. R. Kandel, J. H. Schwartz, T. M. Jessell, S. Siegelbaum, A. J. Hudspeth, S. Mack *et al.*, *Principles of neural science*. McGraw-hill New York, 2000, vol. 4.
- [7] A. Achille, M. Rovere, and S. Soatto, “Critical learning periods in deep networks,” in *International Conference on Learning Representations*, 2018.
- [8] S. Jastrzebski *et al.*, “Catastrophic fisher explosion: Early phase fisher matrix impacts generalization,” in *International Conference on Machine Learning*, 2021, pp. 4772–4784.

[9] A. S. Golatkar, A. Achille, and S. Soatto, "Time matters in regularizing deep networks: Weight decay and data augmentation affect early learning dynamics, matter little near convergence," *Advances in Neural Information Processing Systems*, vol. 32, 2019.

[10] T. K. Hensch, "Critical period plasticity in local cortical circuits," *Nature reviews neuroscience*, vol. 6, no. 11, pp. 877–888, 2005.

[11] E. I. Knudsen and P. F. Knudsen, "Sensitive and critical periods for visual calibration of sound localization by barn owls," *Journal of Neuroscience*, vol. 10, no. 1, pp. 222–232, 1990.

[12] M. Kleinman, A. Achille, and S. Soatto, "Critical learning periods for multisensory integration in deep networks," in *Proceedings of the IEEE/CVF Conference on Computer Vision and Pattern Recognition*, 2023, pp. 24 296–24 305.

[13] T. K. Hensch, "Critical period regulation," *Annual Review of Neuroscience*, vol. 27, no. 1, pp. 549–579, 2004.

[14] G. Yan, H. Wang, X. Yuan, and J. Li, "CriticalFL: A critical learning periods augmented client selection framework for efficient federated learning," in *Proceedings of the 29th ACM SIGKDD Conference on Knowledge Discovery and Data Mining*, 2023, pp. 2898–2907.

[15] Q. Long, Q. Wang, C. Anagnostopoulos, and D. Bi, "Decentralized personalized federated learning based on a conditional ‘sparse-to-sparser’ scheme," *IEEE Transactions on Neural Networks and Learning Systems*, vol. 36, no. 10, pp. 19 160–19 174, 2025.

[16] J. Kang, Z. Xiong, D. Niyato, S. Xie, and J. Zhang, "Incentive mechanism for reliable federated learning: A joint optimization approach to combining reputation and contract theory," *IEEE Internet of Things Journal*, vol. 6, no. 6, pp. 10 700–10 714, 2019.

[17] Y. Shi, H. Yu, and C. Leung, "Towards fairness-aware federated learning," *IEEE Transactions on Neural Networks and Learning Systems*, vol. 35, no. 9, pp. 11 922–11 938, 2024.

[18] Z. Chen *et al.*, "FDFL: Fair and discrepancy-aware incentive mechanism for federated learning," *IEEE Transactions on Information Forensics and Security*, vol. 19, pp. 8140–8154, 2024.

[19] H. Wu, X. Tang, Y.-J. A. Zhang, and L. Gao, "Incentive mechanism for federated learning with random client selection," *IEEE Transactions on Network Science and Engineering*, vol. 11, no. 2, pp. 1922–1933, 2024.

[20] L. Cai, Y. Dai, Q. Hu, J. Zhou, Y. Zhang, and T. Jiang, "Bayesian game-driven incentive mechanism for blockchain-enabled secure federated learning in 6g wireless networks," *IEEE Transactions on Network Science and Engineering*, vol. 11, no. 5, pp. 4951–4964, 2024.

[21] Y. Zhan, P. Li, Z. Qu, D. Zeng, and S. Guo, "A learning-based incentive mechanism for federated learning," *IEEE Internet of Things Journal*, vol. 7, no. 7, pp. 6360–6368, 2020.

[22] Y. Sarikaya and O. Ercetin, "Motivating workers in federated learning: A stackelberg game perspective," *IEEE Networking Letters*, vol. 2, no. 1, pp. 23–27, 2019.

[23] P. Sun *et al.*, "Pain-FL: Personalized privacy-preserving incentive for federated learning," *IEEE Journal on Selected Areas in Communications*, vol. 39, no. 12, pp. 3805–3820, 2021.

[24] P. Bolton and M. Dewatripont, *Contract theory*. MIT press, 2004.

[25] X. Wang, Y. Zhao, C. Qiu, Z. Liu, J. Nie, and V. C. Leung, "InFEDge: A blockchain-based incentive mechanism in hierarchical federated learning for end-edge-cloud communications," *IEEE Journal on Selected Areas in Communications*, vol. 40, no. 12, pp. 3325–3342, 2022.

[26] G. Yu *et al.*, "IronForge: An open, secure, fair, decentralized federated learning," *IEEE Transactions on Neural Networks and Learning Systems*, vol. 36, no. 1, pp. 354–368, 2025.

[27] T. L. Nguyen *et al.*, "Blockchain-empowered trustworthy data sharing: Fundamentals, applications, and challenges," *ACM Computing Surveys*, vol. 57, no. 8, pp. 1–36, Mar. 2025.

[28] M. Kleinman, A. Achille, and S. Soatto, "Critical learning periods emerge even in deep linear networks," in *International Conference on Learning Representations*, 2024.

[29] A. D. Procaccia, H. Shao, and I. Shapira, "Incentives in federated learning with heterogeneous agents," in *The Fourteenth International Conference on Learning Representations*, 2026.

[30] H. Zhao, M. Zhou, W. Xia, Y. Ni, G. Gui, and H. Zhu, "Economic and energy-efficient wireless federated learning based on stackelberg game," *IEEE Transactions on Vehicular Technology*, vol. 73, no. 2, pp. 2995–2999, 2024.

[31] T. Liu, B. Di, P. An, and L. Song, "Privacy-preserving incentive mechanism design for federated cloud-edge learning," *IEEE Transactions on Network Science and Engineering*, vol. 8, no. 3, pp. 2588–2600, 2021.

[32] B. Han *et al.*, "Dynamic incentive design for federated learning based on consortium blockchain using a stackelberg game," *IEEE Access*, vol. 12, pp. 160 267–160 283, 2024.

[33] N. Ding, L. Gao, and J. Huang, "Joint participation incentive and network pricing design for federated learning," in *IEEE INFOCOM*, 2023, pp. 1–10.

[34] G. Huang, Q. Wu, J. Li, and X. Chen, "IMFL-AIGC: Incentive mechanism design for federated learning empowered by artificial intelligence generated content," *IEEE Transactions on Mobile Computing*, vol. 23, no. 12, pp. 12 603–12 620, 2024.

[35] M. Tang, F. Peng, and V. W. Wong, "A blockchain-empowered incentive mechanism for cross-silo federated learning," *IEEE Transactions on Mobile Computing*, vol. 23, no. 10, pp. 9240–9253, 2024.

[36] Z. Wang, Q. Hu, R. Li, M. Xu, and Z. Xiong, "Incentive mechanism design for joint resource allocation in blockchain-based federated learning," *IEEE Transactions on Parallel and Distributed Systems*, vol. 34, no. 5, pp. 1536–1547, 2023.

[37] S. Yuan, H. Lv, H. Liu, C. Wu, S. Guo, Z. Liu, H. Chen, and J. Li, "TradeFL: A trading mechanism for cross-silo federated learning," in *IEEE 43rd International Conference on Distributed Computing Systems (ICDCS)*, 2023, pp. 920–930.

[38] N. K. Jadav, R. Gupta, and S. Tanwar, "Blockchain and edge intelligence-based secure and trusted V2V framework underlying 6G networks," in *IEEE INFOCOM Workshops*, 2022, pp. 1–6.

[39] X. Zhang, F. Li, Z. Zhang, Q. Li, C. Wang, and J. Wu, "Enabling execution assurance of federated learning at untrusted participants," in *IEEE INFOCOM 2020*, 2020, pp. 1877–1886.

[40] E. Yu, Y. Xu, L. Gao, J. Cao, Q. Xiang, and L. He, "R-Manager: Consortium blockchain-based vehicle reputation management for high-quality reports in traffic-oriented crowdsourcing," *IEEE Transactions on Vehicular Technology*, vol. 74, no. 1, pp. 984–999, 2025.

[41] C. Chen, W. Wang, and B. Li, "Round-robin synchronization: Mitigating communication bottlenecks in parameter servers," in *IEEE INFOCOM*, 2019, pp. 532–540.

[42] P. Kairouz *et al.*, "Advances and open problems in federated learning," *Foundations and Trends® in Machine Learning*, vol. 14, no. 1–2, pp. 1–210, 2021.

[43] Z. Wang, L. Gao, and J. Huang, "Multi-dimensional contract design for mobile data plan with time flexibility," in *Proceedings of the Eighteenth ACM International Symposium on Mobile Ad Hoc Networking and Computing*, 2018, p. 51–60.

[44] K. Joseph and M. U. Kalwani, "The role of bonus pay in salesforce compensation plans," *Industrial Marketing Management*, vol. 27, no. 2, pp. 147–159, 1998.

[45] G. A. Churchill, N. M. Ford, O. C. Walker, M. W. Johnston, and J. F. Tanner, *Sales force management*. Irwin Homewood, IL, 1993.

[46] Ahmet Melih Selcuk and Zeynep Muge Avsar, "Dynamic pricing in airline revenue management," *Journal of Mathematical Analysis and Applications*, vol. 478, no. 2, pp. 1191–1217, 2019.

[47] T. Brown *et al.*, "Language models are few-shot learners," *Advances in neural information processing systems*, vol. 33, pp. 1877–1901, 2020.

[48] W. Wang, J. Chen, Y. Jiao, J. Kang, W. Dai, and Y. Xu, "Connectivity-aware contract for incentivizing IoT devices in complex wireless blockchain," *IEEE Internet of Things Journal*, vol. 10, no. 12, pp. 10 413–10 425, 2023.

[49] Z. Zhou, P. Liu, J. Feng, Y. Zhang, S. Mumtaz, and J. Rodriguez, "Computation resource allocation and task assignment optimization in vehicular fog computing: A contract-matching approach," *IEEE Transactions on Vehicular Technology*, vol. 68, no. 4, pp. 3113–3125, 2019.

[50] Y. Zhang, L. Song, W. Saad, Z. Dawy, and Z. Han, "Contract-based incentive mechanisms for device-to-device communications in cellular networks," *IEEE Journal on Selected Areas in Communications*, vol. 33, no. 10, pp. 2144–2155, 2015.

[51] Y. Zhao, Z. Liu, C. Qiu, X. Wang, F. R. Yu, and V. C. Leung, "An incentive mechanism for big data trading in end-edge-cloud hierarchical federated learning," in *IEEE Global Communications Conference (GLOBECOM)*, 2021, pp. 1–6.

[52] "Ganache," [Online]. Available: "<https://archive.trufflesuite.com/ganache>", 2024, (Accessed Jan. 12, 2026).

[53] D. J. Beutel *et al.*, "Flower: A friendly federated learning research framework," *arXiv preprint arXiv:2007.14390*, 2020.

[54] "Web3.py," [Online]. Available: "<https://web3py.readthedocs.io/en/v5>", 2024, (Accessed Jan. 12, 2026).

[55] "FastAPI framework," [Online]. Available: "<https://fastapi.tiangolo.com>", 2024, (Accessed Jan. 12, 2026).

[56] A. Krizhevsky, G. Hinton *et al.*, "Learning multiple layers of features from tiny images," *Technical report*, 2009.

[57] H. Xiao, K. Rasul, and R. Vollgraf, "Fashion-MNIST: A novel image dataset for benchmarking machine learning algorithms," *arXiv preprint arXiv:1708.07747*, 2017.